

Irregular shaping of polystyrene nanosphere array by plasma etching

HAO LUO¹, TINGTING LIU¹, JUN MA¹, WEI WANG², HENG LI², PENGWEI WANG³,
JINTAO BAI^{1,4}, GUANGYIN JING^{1*}

¹Nano Biophotonics Center, National Key Laboratory and Incubation Base of Photoelectric Technology and Functional Materials, Department of Physics, Northwest University, 710069, Xi'an, China

²School of Physics, Peking University, Beijing, 100871, China

³ Northwest Institute for Nonferrous Metal Research (NIN), 710016, Xi'an, China

⁴Institute of Photonics and Photon-Technology, and Provincial Key Laboratory of Photoelectronic Technology of Northwest University, 710069, Xi'an, China

The morphology of nanospheres is crucial for designing the nanofabrication in the nanosphere lithography. Here, by plasma etching, the controllable tailoring of the nanosphere is realized and its morphology dependence on the initial shape, microscopic roughness, and the etching conditions is investigated quantitatively. The results show that the shape evolution strongly depends on the etching gas, power, and process duration. Particularly, the aspect ratio (diameter/height) significantly increases with violent etching, turning the spherical shape into tiny ellipsoidal nanoparticles. The findings are practical to the protocol of non-uniform etching of nanoobjects and provide the useful design tool for the device fabrication at nanoscale.

Keywords: *polystyrene; nanosphere array; self-assembly*

© Wrocław University of Technology.

1. Introduction

As the fabrication techniques of electronic devices are currently switching from microscale into nanoscale, both traditional and novel techniques have been well developed. Optical lithography [1], for example, which strongly depends on the special photomask for diverse micro/nano devices, has been extensively used in semiconductor industry. In order to avoid the using of masks, atomic force microscope (AFM) [2] was designed to manipulate and fabricate the structures down to the nanoscale. By moving the ultrasharp tip, it easily patterns the material into desired structures directly, through either physical control or chemical reaction, however, the technique has its limitations due to reliability and time cost. The maskless methods, such as focused ion beam (FIB) [3], electron beam lithography (EBL) [4] and proton beam writing [5] are

accurate and flexible but usually suffer from the high cost and long production time. Nanosphere lithography (NSL) [6], as a low cost, large-area, novel material nanofabrication technique, based on the self-assembly of nanoparticles into the well-ordered mask, is employed to manufacture versatile nano- and micro-structures, such as micro-electromechanical systems (MEMS) [7, 8], photonic crystals [9, 10], memory devices [11, 12], etc. NSL allows low-cost and controllable nanofabrication, thus attracting tremendous attention.

In the NSL, the periodic particle array (PPA) made from latex (i.e. polystyrene spheres) is primarily functioned as a pre-mask, and can be readily realized via methods such as capillary deposition [13], spin-coating [14], interface assembly [15], etc. Usually, the close-packed nanosphere array is produced by these self-assembly methods, which requires the pattern transfer from hexagonal configuration to other desired structures, such as triangular, rectangular, circular dot array etc.,

*E-mail: jing@nwu.edu.cn

subsequently limiting the NSL for versatile structure fabrication. During the transformation of the close-packed template to the final structures, shaping individual nanospheres by heating [16, 17] and etching [18, 19] plays an important role. Heating leads to the melting of the soft spheres PPA, then shrinking or deforming into the netlike structure, which tunes this 2-D array. In contrast, the etching method aims to adjust the size of the individual sphere. C. Cong *et al.* [17] designed the regular holes with rectangular and circular shapes by both heating and etching, and also obtained neck-like structures by plasma etching. As reported by Y. H. Ting *et al.* [20], Ar/O₂ was used to etch the polymer film to study the effects of the aggregation and cross-linking diblocks of polymer films on surface roughness. By examining the optical properties of PPA nanospheres, T. Fujimura *et al.* [21] observed the irregular modification of polystyrene (PS) nanospheres (aspect ratio $\neq 1$) during the reactive ion etching, and found that this symmetry-breaking affected the optical properties of the nano-array. When manufacturing hierarchical nanoparticle arrays, D. Xia *et al.* [22] observed, with a scanning electron microscope (SEM), the etched PS spheres which had a rough top and elliptical shape. As the uniformity of the sphere array and the controllable shape of the individual spheres are highly desirable for device applications it is important to understand the etching process for the nanoscale template or mask made from the nanospheres arranged in the well-ordered way. Although the PPA has been developed by various self-assembly methods and etching processes, the shape evolution of the sphere by tailoring morphology (i.e. aspect ratio) has not been well investigated so far, and the anisotropy (i.e. sphere or ellipse) has not been widely discussed as well. Moreover, the refined surface roughness of the nanosphere after shaping needs to be examined quantitatively.

In this work, we investigate the effect of process parameters such as plasma etching power, gas flow, substrate material, type of etching gas, on the shape and roughness of a nanosphere. By varying systematically the key parameters, the dependence of the diameter to height ratio of the nanosphere on the etching conditions is established.

2. Experiments

2.1. Self-assembly of PAA template

Before the etching process, spheres of nanometer size were initially spread onto a substrate to obtain close-packed monolayer coverage. The polystyrene sphere is a good candidate for plasma etching, due to its polymer nature, commercial accessibility, and the wide range of applications in the NSL technology. Aqueous suspension of polystyrene nanospheres (10 % w/v in concentration, 762 nm in diameter, GmbH, Germany) were nicely monodispersed (coefficient variation < 5 %) and used as received. Note that the monodispersity of nanospheres is a key factor to produce the uniform 2D colloidal crystal layer, and significantly influences the quality of the nanosphere array during the etching process. The solid content of the colloidal solutions was diluted to about 5 % w/v by adding ethanol. The solution drop was introduced onto the air/water interface vertically by using a pumping syringe. In this process, the drop of solution should be located just above the air/water interface, considering the fact that pushing the solution drops onto the interface leads the suspension and water surface to merge. Then the nanospheres spontaneously spreaded along the air/water interface and aggregated into a regular close-packed structure. In our case, the nanospheres were taken apart from each other, in order to measure their dimensions in the AFM system. Thereafter, clean silicon and glass substrates were covered by the nanosphere monolayer film by picking up the nanosphere film floating at the interface.

2.2. Plasma etching

Subsequently, the dry nanosphere films were transferred into a plasma system (FEMTO Beispiel Variante A, Diener, Germany) and etched under different conditions. The dielectric constant of the substrate affected the local electric field between two electrodes of the plasma system, thus possibly causing variation in the etching process. Consequently, two substrates were selected to support the nanospheres, i.e. glass and silicon substrates. During the plasma etching, the influence of gas type

and flow rate, etching power and etching time were examined. The etching was performed by introducing air, and then Ar/O₂ for comparison. Etching duration, power, and gas flow were varied in the ranges of 0 – 30 min, 25 – 55 W, and 10 – 20 sccm, respectively. Scanning electron microscope (SEM, Nano430, FEI) was employed to image and measure the in-plane (X-Y) dimension of the spheres. AFM (Dimension Icon, Veeco) was used to examine the surface roughness of the spheres obtained under different etching conditions. Due to the high resolution in the vertical direction (Z-axis) in the AFM system, the height of the sphere can be determined with a high accuracy whereas, the topography images of AFM are inevitably deformed in the in-plane direction. In summary, we used SEM to get the in-plan size and AFM to get the vertical size of the nanospheres, and then we were able to assess accurate shapes of the nanospheres.

3. Results and discussion

3.1. Effect on in-plane size of the nanosphere

The heterogeneity of the spheres, local electric field and even their mutual interaction, are possibly responsible for the irregular plasma etching of the polymer spheres, for which all, the in-plane shape is a suitable measure. As shown in Fig. 1, the spheres get smaller and smaller with the progress of etching. The shape of the sphere is perfectly spherical at the beginning, and loses its circular shape after longer etching (Fig. 1(e) – (f)). As indicated by dot lines in Fig. 1(e) and 1(f), some spherical particles are transferred into ellipses with random orientation, whereas others maintain the spherical cap. The major-axis/minor-axis aspect ratio reaches about 1.2. Additionally, the irregular shape of the sphere occurs as pointed by the arrows in Fig. 1(e).

In shaping the nanospheres, the transition from circle to ellipse, even polygon, is complicated for three reasons. Firstly, the initial shape of each sphere obviously affects its final shape. Secondly, the different roughness of the sphere surface inevitably contributes to the lack of high symmetry [23]. Materials subjected to a typical plasma

etching usually exhibit microscopic bulges and pits along the particles resulting in etching differences [24]. In present polymer beads, uneven parts of particles were exposed to the much larger actual contact area with the plasma gas in comparison with the flat parts of the particles. Under the same etching condition, the rough parts were carved out violently, which resulted in the short dimension in this direction. Thirdly, another source of this symmetry-breaking comes from the non-uniformity and disturbances of the etching system.

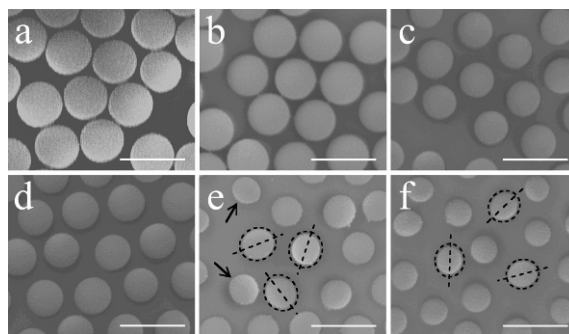


Fig. 1. SEM images of the PS spheres on Si substrates etched under 10 sccm air flow and 40 W power for different periods of time, (a) 0 min, (b) 6 min, (c) 10 min, (d) 12 min, (e) 15 min, and (f) 18 min. All of the scale bars are 1 μm .

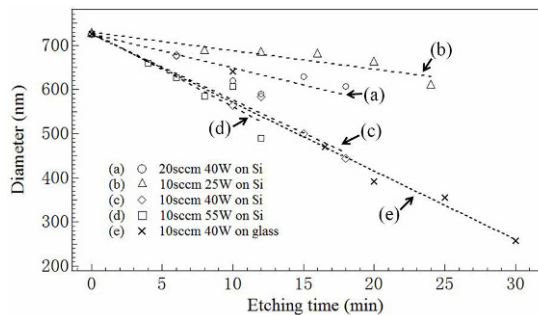


Fig. 2. Dependence of PS spheres diameter on the etching time under different etching conditions indicated by different types of marks. All the dot lines are the linear fittings of the data points.

The relations between a sphere diameter (in-plane) and etching time, under different conditions, are plotted in Fig. 2. To determine the diameter, a

number of spheres were examined in the SEM images for both the perfect spherical and ellipsoidal ones, and the average values were taken. Under the same gas flow rate (10 sccm) and using the same substrate (silicon), the spheres were etched much faster at the power of 40 W than that of 25 W, but the further increase of the power raised the etching rate only slightly, as indicated in Fig. 2, so as the etching rate at 55 W was comparable to that at 40 W. When the etching was carried out at 25 W, the glow was unstable and twinkled heavily in the reaction chamber, due to glow discharge instability. A critical power (here 40 W) is believed to give stable glow and saturated etching rate. On the other hand, the results show that the substrate effect on the etching process is not obvious, since the etching rate of about 16.3 nm/min on glass (dot line (e)) is very close to 16.0 nm/min on silicon (dot line (c)) (Fig. 2). Moreover, the gas flow increase from 10 sccm to 20 sccm, results in halving the etching rate correspondingly. In general, the dependence of the etching rate on the etching duration reflects the scaling law of $D \propto t^{-1}$. The etching rate is inversely proportional to the gas flow, and saturates at a certain plasma power.

3.2. Effect on surface roughness

To focus on an individual bead, we used AFM to study the effect of plasma etching on the surface roughness of the nanospheres. Fig. 3 shows the AFM topography images of individual spheres, etched for different durations. The root mean square of the roughness, derived from the AFM analysis, was used to characterize the surface roughness. As shown in Fig. 4, the surface roughness shows a tendency to rising during the early stage, until a maximum and then is dropping for the longer etching time.

Etchant redistribution [1] and shadowing effect [23] were introduced to describe the surface variation in a typical etching process for the bulk and film materials. The etchant from the plasma flow hits the microscopic inclined surface (rough surface), and some amount of the etchant is rebound, which results in the redistribution of this etchant. This redistribution leads to enhanced trans-

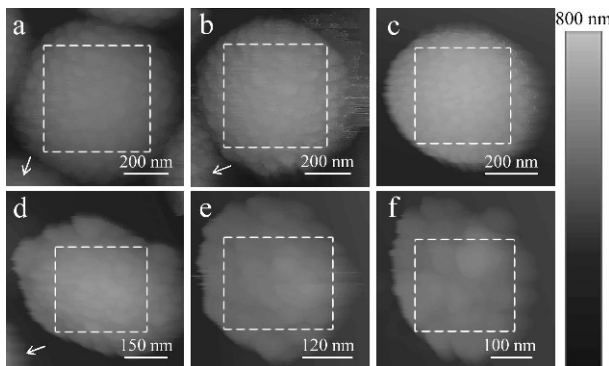


Fig. 3. AFM topography images of the single PS spheres on Si substrate, etched under 10 sccm air flow and 40 W power, after etching for (a) 0 min, (b) 6 min, (c) 10 min, (d) 12 min, (e) 15 min, and (f) 18 min. The dotted boxes are the areas of the roughness measurements, the arrows indicate the neighboring spheres.

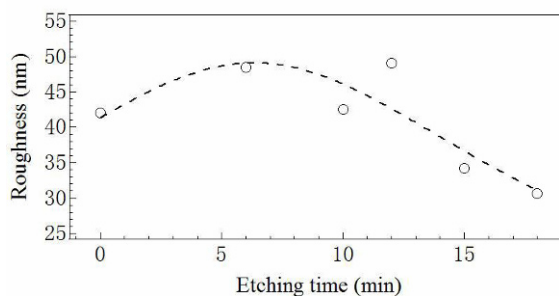


Fig. 4. Roughness of the individual sphere vs. etching time. The samples were etched under 10 sccm air flow and 40 W power. The dot line is fitted by a Gaussian function for eye guide line.

fer of the etchant to the “valleys”, which as a consequence, contributes to the increase of surface roughness, demonstrating the rising tendency, shown in Fig. 4. The shadowing effect means that the “peaks” hinder the access of both the etchant and the deposited atoms to the “valleys”. The blocking effect is more obvious for atoms deposited under ideal conditions [25], where the increase of the height of the “peaks” is associated with an increase in roughness. However, because the flowing gas reduced the deposition during our etching process, the etching of “peaks” was relatively more violent. Summing up, when the roughness increases to a critical level, the “peaks” pro-

tect the “valleys” from etchant, thus reducing the surface roughness, which shows the dropping tendency as in Fig. 4.

3.3. Effect on aspect ratio

On the basis of the discussion above, the in-plane dimension (average diameter) has been determined, which raises the question whether the vertical sphere height has the same value as the horizontal diameter or is just comparable with that in-plane (to say, aspect ratio $\neq 1$). Fig. 5 shows the AFM topography images of the nanospheres etched under 10 sccm gas flow at 40 W power on Si substrate, for the different durations. As is known, the AFM image is obtained by moving a very sharp tip laterally and vertically to image the 3D morphology of the sample. The smaller the tip is, the closer the real morphology of the sample can be imaged. However, the curvature radius of the tip is limited which results in the broadening of the sample dimensions measured in the scanning direction or in-plane: this is known as “tip effect” [26]. Therefore, the AFM images (Fig. 5) look different from the corresponding SEM images (Fig. 1), and can lead to deviation in-plane of measured dimensions. To avoid the uncertainty of the height measurement caused by the tight distribution of the adjacent spheres, isolated spheres were located in the AFM system within a suitable zoom-in range. The topography images of the spheres obtained at different etching times are displayed in Fig. 5, and the values of sphere height in the vertical direction are plotted in the Fig. 6(a). It is notable that the AFM images of the spheres obtained in a short etching time display the nice circular perimeter (Fig. 5(a) – (c)), while the morphology of those spheres under heavy etching shows rather irregular shape (Fig. 5(d) – (f)). Interestingly, under this condition, the etching rate of a sphere along the Z-axis direction is larger than that in the X-Y direction, namely the height becomes smaller than the transverse size. The aspect ratio of the sphere (represented by circle marks and dashed line in Fig. 6(c),) increases linearly with the etching time.

Usually, a gas mixture [27, 28] (i.e. Ar/O₂) is used for the etching of latex, which can gently

tailor the particles, thus the aspect ratio has been rarely discussed in the literature. However, etching in a simple gas, for example air, can be performed rather than in Ar/O₂, due to its low cost. Here, in order to explore the etching under the air flow, and illustrate the difference of this etching from that using Ar/O₂, the experiments of etching in air flow were carried out. The etching rates in X-Y plane, calculated from Fig. 6(a) and 6(b), are 16.0 nm/min and 11.5 nm/min, in air and Ar/O₂ respectively, while those in the Z direction are 31.2 nm/min and 16.8 nm/min, respectively. These results demonstrate that the etching is more violent under air flow than under Ar/O₂, and the etching using air leads to highly irregular shapes (Fig. 6(c)).

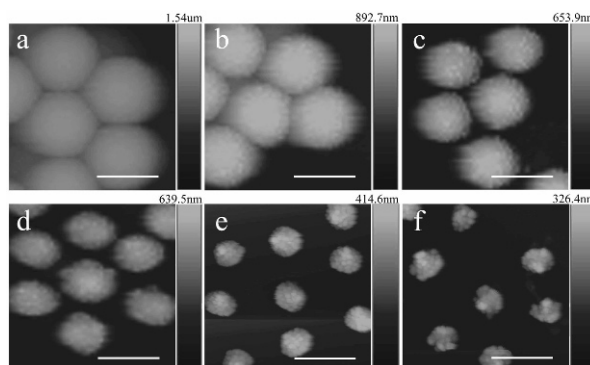


Fig. 5. AFM images of PS spheres array on Si substrate etched under 10 sccm air flow and 40 W power, for 0 min (a), 6 min (b), 10 min (c), 12 min (d), 15 min (e), and 18 min (f). All the scale bars are 700 nm.

To analyze the relations between the air gas flux and power on the aspect ratio of the etched spheres, additional experiments were performed and the results are listed in the Table 1. As indicated in the Table 1, the plasma power plays a negligible role in controlling the aspect ratio during etching (i.e. aspect ratio is 1.2 and 1.3 for the power of 25 and 55 W, respectively). On the other hand, the aspect ratio of the spheres significantly increases to 2.1 when the gas flux increases from 10 sccm to 20 sccm, which means that the nanosphere has been shaped into a flat cap. As the gas flow increases, the number of gas molecules in reaction chamber also increases, which leads to higher density of the etchant, thus causing an increase in the

Table 1. Influence of the gas flow, power on the aspect ratio during the etching process.

Number	Gas flux [sccm]	Power [W]	Duration [min]	Diameter [nm]	Height [nm]	Aspect ratio [D/H]
Sample 1	10	25	24	608	503	1.2
Sample 2	10	55	10	606	471	1.3
Sample 3	20	40	18	607	286	2.1

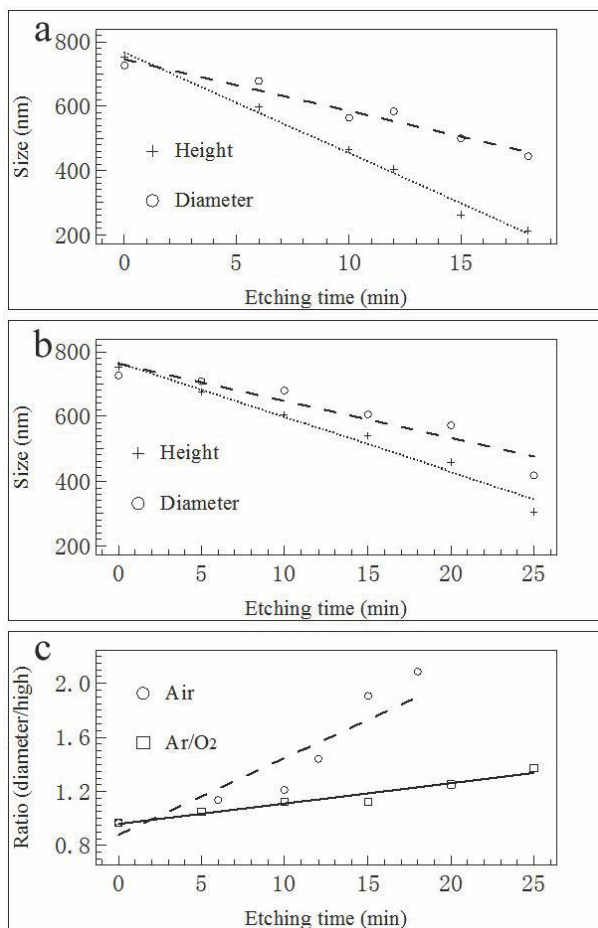


Fig. 6. Sphere dimension evolution with the etching time, under air etching (a), Ar/O₂ etching (b); and dependence of the aspect ratio on etching time (c).

etch rate and aspect ratio. In the electric field, the etchant moves along Z-axis, so the etching reaction in the Z-axis direction is more intense. Moreover, in the X-Y plane, the spheres are arranged in a regular array closely, therefore, the adjacent nanospheres reduce the flow of gas and exchange

of material [24, 29], which accounts for the irregular shaping during the etching.

4. Conclusions

To controllably shape the nanospheres towards a periodic particle array and investigate the symmetry-breaking of the nanosphere array by plasma etching, irregular shaping is defined and its dependence on the etching condition is systematically determined in a quantitative way. We have stated that the in-plane dimension of the sphere linearly decreases with the etching duration and that after longer etching, some spheres transform into ellipses which have a random orientation. Moreover, the gas flow plays a more important role in regulating the relation between the diameter of etched sphere and etching time than the material of substrate. When the etching power reaches a critical level, the etching rate becomes saturated. Furthermore, the surface roughness of individual sphere exhibits a tendency to rising during the early stage of etching, then drops with increasing etching time. Plasma etching in air has stronger effect on the aspect ratio than Ar/O₂ plasma etching. The aspect ratio of PS spheres shaped by air plasma etching can be easily tuned from about 1 to 2.2, by increasing the etching time. At last, we have found that the gas flow is a pivotal parameter to control the aspect ratio during air plasma etching.

Acknowledgements

The authors gratefully acknowledge the support by NSFC (No. 11104218), Natural Science Basic Research Plan in Shaanxi Province of China (Program No. 2010JZ001), Scientific Research Foundation for the Returned Overseas Chinese Scholars (Shaanxi Administration of Foreign Expert Affairs, 2011).

References

- [1] ZHAO Y., DROTAR J., WANG G, LU T., *Phys. Rev. Lett.*, 82 (1999), 4882.
- [2] HEADRICK J., ARMSTRONG M., CRATTY J., HAMMOND S., SHERI B., BERRIE C., *Langmuir*, 21 (2005), 4117.
- [3] MATSUI S., KAITO T., FUJITA J., KOMURO M., KANDA K., HARUYAMA Y., *J. Vac. Sci Technol.*, 18 (2000), 3181.
- [4] VIEU C. et al., *Appl. Surf. Sci.*, 164 (2000), 111.
- [5] VAN KAN J., BETTIOL A., WATT F., *Nano Lett.*, 6 (2006), 579.
- [6] HAYNES C., VAN DUYN R., *J. Phys. Chem. B*, 105 (2001), 5599.
- [7] DAMEAN N., PARVIZ B., LEE J., ODOM T., WHITESIDES G., *J. Micromech Microeng*, 15 (2004), 29.
- [8] M. CHASON, A. SKIPOR, A. TUNGARE, D. GAMOTA, AND S. GHAEM, *Google Patents*, US Patent 6, 649 (2003), 852.
- [9] GULDIN S. et al., *Nano Lett.*, 10 (2010), 2303.
- [10] FU W., WONG K., CHOI H., *J. Appl. Phys.*, 107 (2010), 063104.
- [11] S.WEEKES, F. OGRIN, AND W. MURRAY, *Langmuir*, 20 (2004), 11208.
- [12] ALEXE M., HARNAGEA C., HESSE D., GOSELE U., *Appl. Phys. Lett.*, 75 (1999), 1793.
- [13] LI H., MARLOW F., *Chem. Mater.*, 18 (2006), 1803.
- [14] JIANG P., MCFARLAND M., *J. Am. Chem. Soc.*, 126 (2004), 13778.
- [15] MOON G. et al., *ACS Nano*, 5 (2011), 8600.
- [16] OKUBO T., *J. Chem. Phys.*, 95 (1991), 3690.
- [17] CONG C., JUNUS W., SHEN Z., YU T., *Nanoscale research letters*, 4 (2009), 1324.
- [18] YAN L., WANG K., WU J., YE L., *Phys. Chem. B*, 110 (2006), 11241.
- [19] LI Y., LEE E., CAI W., KIM K., CHO S., *ACS Nano*, 2 (2008), 1108.
- [20] TING Y., LIU C., PARK S., JIANG H., NEALEY P., WENDT A., *Polymers*, 2 (2010), 649.
- [21] FUJIMURA T., TAMURA T., ITOH T., HAGINOYA C., KOMORI Y., KODA T., *Appl. Phys. Lett.*, 78 (2001), 1478.
- [22] XIA D., KU Z., LI D., BRUECK S., *Chem. Mater.*, 20 (2008), 1847.
- [23] DROTAR J., ZHAO Y., LU T., WANG G., *Phys. Rev. B*, 62 (2000), 2118.
- [24] CHAN W., CHASON E., *J. Appl. Phys.*, 101 (2007), 121301.
- [25] YAO J. , GUO H., *Phys. Rev. E*, 47 (1993), 1007.
- [26] ABRAHAM F. F., BATRA I. P., CIRACI S., *Phys. Rev. Lett.*, 60 (1988), 1314.
- [27] ZHANG G., WANG D., MOHWALD H., *Nano Lett.*, 7 (2007), 3410.
- [28] TING Y. et al., *J. Vac. Sci Technol.*, 26 (2008), 1684.
- [29] WU P., PENG L., TUO X., WANG X., YUAN J., *Nanotechnology*, 16 (2005), 1693.

Received 2013-01-16
Accepted 2013-03-03